Electronic structure calculations and physicochemical experiments quantify the competitive liquid ion association and probe stabilisation effects for nitrobenzospiropyran in phosphonium-based ionic liquids.

Simon Coleman[1], Dermot Diamond[1,2], Damien Thompson[3*] and Robert Byrne[2]**

[1] Biomedical Diagnostics Institute, National Centre for Sensor Research, Dublin City University, Dublin 9, Ireland
[2] CLARITY: Centre for Sensor Web Technologies, National Centre for Sensor Research, Dublin City University, Dublin 9, Ireland
[3] Tyndall National Institute, University College Cork, Cork, Ireland
*Corresponding author: damien.thompson@tyndall.ie
**Corresponding author: robert.byrne@dcu.ie

Abstract

Liquid ion-pair (LIP) formation in ionic liquids (ILs) has been examined using a series of electronic structure calculations that measure the relative extents of ion pairing and probe stabilisation for the photochromic dye nitrobenzospiropyran (**BSP**) in phosphonium-based ILs with both $[Cl]^-$ and $[NTf_2]^-$ anions. Physicochemical properties of the liquids were measured experimentally by adding **BSP** and monitoring its photochromic properties within each liquid. Taken together, the computed complexation energies and measured spectroscopic properties support recent Walden plots of conductivity-viscosity behaviour obtained for the same ILs and reveal the atom-scale structure and energetics that underly the observed transport properties. LIP formation was significantly stronger in $[P_{6,6,6,14}][Cl]$ resulting in effectively neutral liquid components. This was reflected in the measured $\Delta S^{\ddagger}$ and E_a values of -96 $J.K^{-1}.mol^{-1}$ and +72 $kcal.mol^{-1}$ respectively. By contrast, the measured $\Delta S^{\ddagger}$ and E_a values in $[P_{6,6,6,14}][NTf_2]$ of -15 $J.K^{-1}.mol^{-1}$ and +85 $kcal.mol^{-1}$ respectively, together with the lower calculated complexation energies, reflect the lower driving force towards LIP formation with the weaker anion. Furthermore, activation barriers to cation diffusion promote LIP relative to competing probe stabilisation interactions. The transport properties of ILs may thus be controlled by a prudent choice of IL

molecular structure, with both the polar hydrophilic headgroup and non-polar hydrophobic tail of the constituent ions serving as distinct targets for rational design.

Introduction

Liquid ion pair (LIP) formation is a ubiquitous feature of ionic liquids (IL) and its extent influences the viscosity and transport properties of the IL solvent. ILs, in contrast with conventional molecular solvents, can form persistent, relatively long-lived nanostructured domains, which mediates their properties or "ionicity" and endows favourable properties upon ILs that make them more suitable than molecular solvents for many applications. Exploitable IL properties can include high thermal stability, negligible vapour pressure and wide electrochemical window.[1-4] The liquid nanostructured domains are dynamic and composed of interchangeable IL components, yet can persist over long time and length scales. More discrete structuring, at the level of individual cation and anion pairs, may play an important role as precursor to the formation of nanostructures and will influence their atom-scale features. The routine implementation of ionic liquids (ILs) as "designer" solvents with user specified properties is therefore an attractive prospect with respect to many applications in the chemical sciences, but their effectiveness will depend to a large degree on harnessing the properties that afford these liquids their unique properties. These fundamental properties originate from nano-scale structural features mentioned above, which are not easily characterised by experiment alone, but provide the basis for unique macroscopic effects, known as the "ionic liquid effect" and "ionicity", that seem to be observed solely in ILs.[5] Since ILs consist *entirely* of ions whose unfavourable packing allows them to form molten salts at conditions near ambient (under 100 ºC for room temperature ILs), the effects observed are clearly related to this set of inherent properties. Applications in fields as diverse as recyclable solvents,[6] catalysis,[7] electrochemistry,[8] synthesis[9] and elemental analysis[10] are all made possible by IL-mediated interactions which do not exist in conventional molecular solvents. To determine the extent to which these "ionicity" effects exist within ILs, the physico-chemical properties must be measured, which in turn allows for systematic isolation of the unique and critical properties that govern these effects. Recent studies of ILs have concluded that evaluation of ILs under the assumption that they behave similarly to molecular solvents is inaccurate and does not encompass the

majority of the liquid properties.[11, 12] ILs are now described as complex media which contain distinct regions which each have specific properties and combine to form the bulk properties of the liquid system. An example of this is the approximation of solvent polarity within ILs. Polarity is a macroscopic property that assumes the entire solvent system acts as a homogeneous medium (like a conventional organic solvent) rather than a medium that may possess distinct nano-structured regions with dramatically different characteristics (like ILs).[13, 14] Therefore, it is understandable that while traditional polarity probes such as Reichardt's dye 30 can provide information about the polarity of organic solvents, this approach fails with the more complex ILs. This is because such probe dyes with permanent dipoles will preferentially locate in localised polar nano-domains within ILs and thus report similar findings despite the wide variations in the characteristics of the surrounding non-polar domains. Hence the observed bulk properties of the ILs are often significantly at variance with expectations arising from these polarity estimations. For this reason, until recently, ILs were believed to have almost uniform polarity similar to that of ethanol or acetonitrile. Our recent studies have shown this estimation to be incorrect by the use of more sophisticated spirocyclic solvatochromic probes that can be switched photonically between polar and non-polar states, enabling the probe molecule to migrate spontaneously between polar/non-polar IL nano-structured domains.[11, 12] The resulting thermodynamic and kinetic parameters confirmed that ILs have a range of properties which cannot be characterised via traditional polarity measurements employed for conventional molecular solvents.

The solvatochromic compound nitrobenzospiropyran (**BSP**) forms the zwitterionic isomer merocyanine (**MC**) when exposed to UV irradiation which allows its use in the measurement of solvent interactions similar to those measured using Reichardt's dye 30. However, the **MC** form is thermodynamically unstable and normally relaxes back to its closed, uncharged spiro (**SP**) form. Thus, the resulting changes in conformational/charge state make this probe far more applicable to IL characterisation, due to its ability to interact with distinct regions within the liquids, unlike previous dyes employed. The **BSP** photoswitching mechanism involves UV-triggered irradiation (typically around 365-375 nm) cleavage of the sp_3 hybridised carbon, C_{spiro} of the indoline ring. Figure 1a shows the structure of spirocyclic compounds and the photoswitchable spiropyran compound in its **BSP** and **MC** states. The **MC** isomer arises from cis-trans isomerisation of the molecule that creates a planar, zwitterionic molecule with charge delocalised across the molecule, as shown in (Figure 1a). The photoswitchable system is a reversible, first order process, wherein irradiation with white light or thermal reversion can result in ring closure to the more stable **BSP** form. Thermal reversion is the process whereby **MC** spontaneously uses heat from its surroundings to receive sufficient energy for the reorientation to occur in the absence of visible light. In addition to photoswitching, the **MC** isomer is found to be sensitive to its molecular environment, with both specific and non-specific solvent interactions mediating the compound's equilibrium between both isomers.[15-18] Generally, for **BSP** in molecular solvents, rate constants increase with decreasing polarity.[19, 20] This is consistent with trends in estimated Kamlet-Taft parameters, which indicate that decreasing levels of hydrogen bonding between solvent and **BSP** results in reduced stabilization of the **MC** form.[11]

(a)

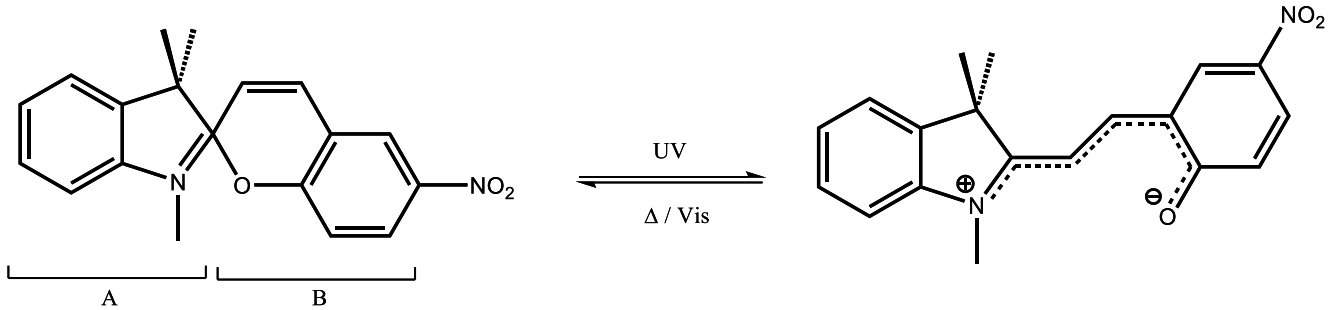

Spiropyran (**BSP**)

Merocyanine ($\mathbf{MC_{BSP}}$)

(b)

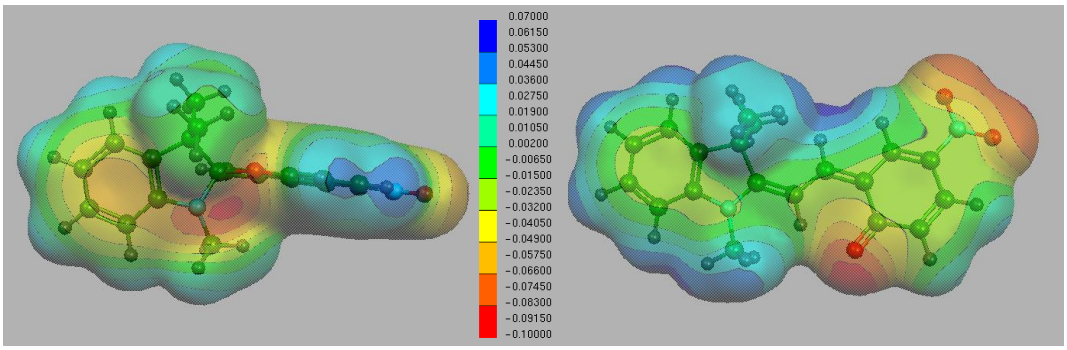

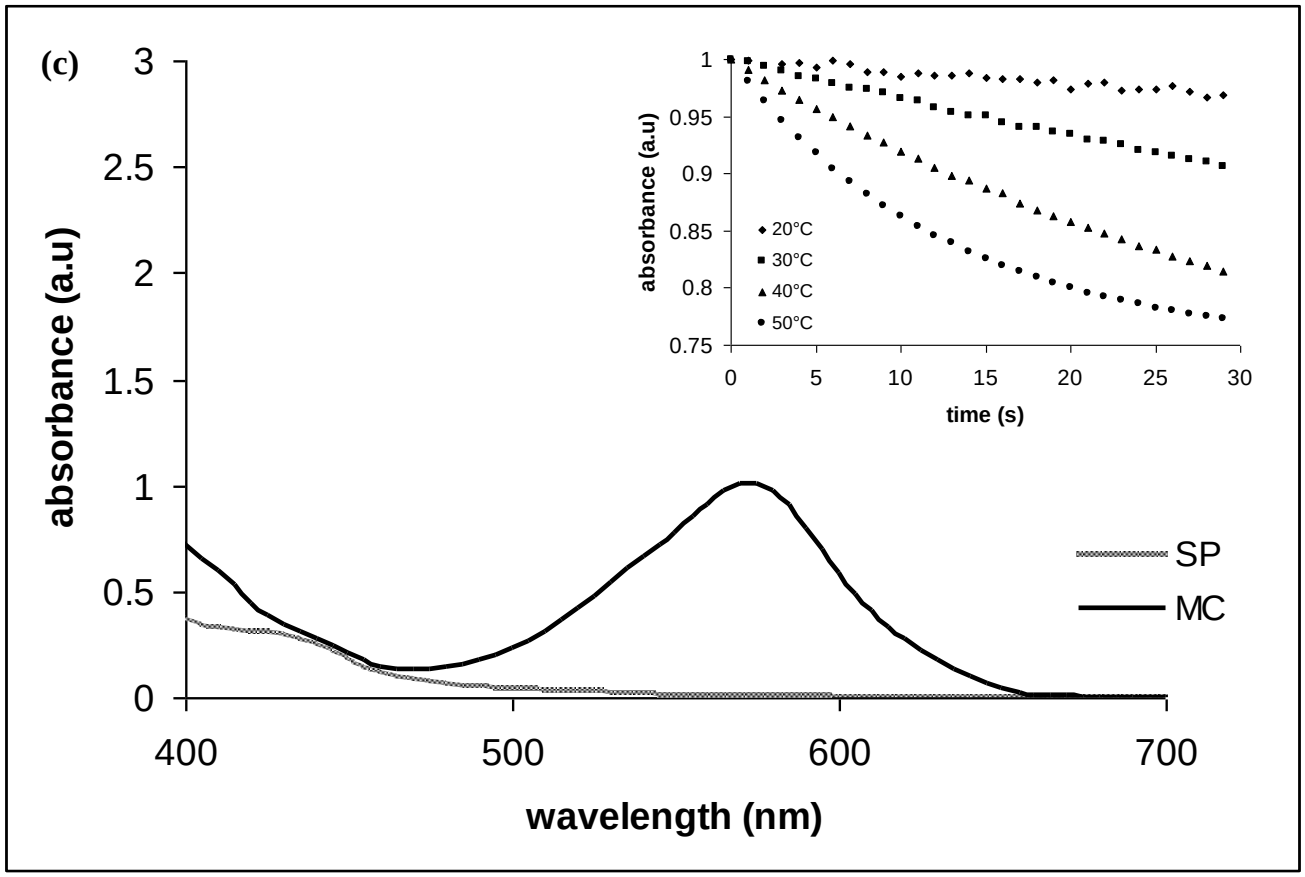

Figure 1. (a) Structure of spirocyclic compounds. Indoline (A) and pyran (B) ring and its photo-switchable states, **BSP** and **MC**. Panel **(b)** shows computed **BSP** and **MC** structures, overlaid with Molecular Electrostatic Potential (MEP) surfaces generated as described in the text and with surfaces coloured according to regions of net charge as marked in the scale bar from -0.10 to +0.07 atomic units **(c)** UV-Vis spectra of spiropyran in its open (**SP**) and closed (**MC**) forms. Inset shows thermal dependence of spiropyran thermal relaxation from which thermodynamic parameters may be derived.

We recently reported the photo- and solvatochromic properties of **BSP** in ILs containing the $[NTf_2]^-$ anion and showed that the kinetics and thermodynamics of the **BSP**-**MC** equilibrium was sensitive to the nature of the cation[20]. Cation-based interactions inhibit the **MC** conversion back to the **BSP** isomer, and may include through-space orbital interactions, that may be specific to the $[C_2mIm]^+$ cation[16], as well as more general electrostatic interactions. Contemporaneous studies suggest that ILs may form ordered systems resembling pseudo-crystalline systems based on stacking of mutual charges (aggregation) or ordered association of cation species to surrounding anions and vice versa.[21-23] Lopes

et al examined the formation of nanostructured domains in ILs containing the imidazolium cation and found that certain imidazolium cations in ILs can be divided into two specific regions: a polar head group where the ion charge resides and a non-polar region where alkyl side-chains extend into space.[24] The association of charged regions by electrostatic interactions is believed to form polar domains within the liquids while non-polar domains are formed by steric packing of alkyl chains. Similar structuring has also been reported for more extensively alkylated systems such as quaternary phosphonium and ammonium based ILs.[23, 25]

To date, the majority of liquid-structure studies have focused on the bulk properties of ILs and examined how the formation of domains influences the overall transport properties of the liquids. However, very short-range, specific intra-molecular interactions that occur between the anion and cation may be crucial to the unique effects found within ILs and these atom- and nano-scale interactions may underlie the formation of the IL-specific bulk properties. The present study exploits this link between the atomic, nano and macro scales for the characterisation of IL bulk properties using **BSP**. Although thermal relaxation has provided insight into the proposed nano-structuring of the liquids, minor inconsistencies have been observed which could not be explained from expected solvent-solute interactions. When ILs are examined at a molecular level, the concept of liquid ion-pairs (LIPs) becomes an important parameter in understanding the properties of ILs, and may explain the origin of such thermodynamic inconsistencies. Specific intra-molecular interactions may provide subtle but important effects upon solute introduction that serve to elucidate further the structuring of the liquid domains. The **MC** isomer of the probe molecule provides a zwitterionic system that can interact with the opposing charges found on each ion of the ILs. As thermal relaxation occurs, ion interactions at each charge site in the molecule would be expected to stabilise the zwitterion. However, the formation of ion-pairs in the liquid itself may offset probe stabilisation, resulting in a competition, or

"tug of war", between inter (**MC**-ion) and intra (ion-ion) interactions. The ability of the ILs to form tightly-bound LIPs may therefore reduce the ability of the liquid to interact with solutes and thus mediate the ionicity and overall effects observed. Since **MC** is sensitive to such interactions, the thermodynamic and kinetic parameters can quantify such liquid properties and explain the processes at work.

To further understand these three-way effects observed between **BSP** and the IL ions, electronic structure calculations were used to quantify the competitive probe-ion and ion-ion interactions. The calculated interaction strengths ΔE for each individual ion's interaction with both **MC** and its solvent counterion provide a quantitative indication of the level of interaction occurring in each case. This allowed for the extent of the competition between probe-ion and ion-ion interactions ΔΔE to be quantified and compared to the observed physicochemical properties. Following the findings of previous studies,[26, 27] two phosphonium based ILs were chosen based on their Walden plot values to determine the effects of ion-pair formation upon the properties of the ILs. Trihexyltertadecylphosphonium Chloride; $[P_{6,6,6,14}][Cl]$ and Trihexyltertadecylphosphonium bistrifluoro(sulfonyl)imide; $[P_{6,6,6,14}][NTf_2]$ were chosen due to the large contrast in anticipated effects due to the more localised charge on $[Cl]^-$, meaning $[P_{6,6,6,14}][NTf_2]$ is expected to be more weakly bound and with more ion mobility. The theoretical models were used to determine if the formation of the charged **MC** form could compete with the charge site of the cation and anion. Preservation of the IL nanostructure, with LIP formation predominating over solute stabilisation, is essential to maintain the transport properties within the liquids and avoid significant local fluctuations; on the other hand, solvent-mediated biasing of photo-switchable equilibria could be a useful sensor design feature.

Experimental

Electronic structure calculations: IL and ion-probe electronic structures were obtained for the systems listed in Table 1 using the Gaussian03 program[28] with the B3LYP hybrid HF-DFT functional[29] and 6-311++G** basis sets. Stable geometries were obtained via nuclear relaxation to root mean square (RMS) atomic forces and displacements below 0.0003 and 0.0012 a.u. respectively, followed by electronic structure determination using the gfoldprint and POP=FULL keywords to generate output files formatted for molecular electrostatic potential (MEP) visualisation using MOLEKEL unix version 4.3.[32] All atomic charges were computed using a natural population analysis (NPA).[30] The basis set used is larger than in previous studies of IL structures and also uses the complete $[P_{6,6,6,14}]^+$ side-chains which were previously truncated to four carbon length chains to reduce calculation costs.[26] Some calculations were repeated using the MP2 method to include electron correlation effects.[31] The MP2 method is far more computationally demanding than B3LYP and so we restricted its use to the two smallest complexes, namely MC:$[Cl]^-$ and MC:$[NTf_2]^-$. As shown in Supporting Information, while the more detailed MP2 method provides as expected closer van der Waals's contacts via the more explicit, and possibly overestimated treatment of dispersion forces and so stronger ΔE values,[33] the general features of the probe-ion complex geometries are preserved and the anion-dependent complexation energy difference $\Delta\Delta E$ is similar for both methods.

Physicochemical experiments: Trihexyl,tetradecyl Phosphonium Chloride (Cytec industries, Niagara, Canada) and Trihexyl,tetradecyl Phosphonium bistrifluoro(sulfonyl)imide (Sigma Aldrich) were purified using previously reported techniques[34] and were stored under argon to exclude uptake of water. Spectrometric studies were carried out using a Cary 50 UV-Vis spectrometer (JVA Analytical, Dublin, Ireland) with temperature controller and fibre optic reflectance probe accessory. Samples were irradiated with UV light at 375nm using an in-house

fabricated array of UV LEDs (Roithner Lasertechnik, Vienna, Austria). Reichardts dye 30 (Sigma-Aldrich chemicals) and 6-Nitro-1',3',3'-trimethylspiro[2H-1-benzopyran-2,2'-indolin] 1',3'-Dihdro-1',3',3'-trimethyl-6-nitrospiro (**BSP**) (Sigma-Aldrich chemicals) were used as purchased with no further purification.

Results and Discussion

Computed properties for the range of IL and ion-probe complexes considered in the present study are given in table 1 below. Comparison of the inter-ion distances in each IL pair with the ion-probe distances, together with the computed complexation energies, provides a quantitative analysis of the strength of ion pairing for intra-IL interactions and the competitive arrangement of the IL ions around the zwitterionic **MC** probe molecule.

Table 1. Computed IL and ion-probe electronic structures.

Complex	Close contact distances (Å)	ΔE (eV)	Δq (a.u)
$[P_{6,6,6,14}]^+ : [Cl]^-$	2.4, 2.4, 2.7 ($H_{CH2} : Cl$); 3.8 ($P : Cl$)	-3.54	-0.09
$[P_{6,6,6,14}]^+ : [NTf2]^-$	2.2 ($H_{CH2} : N$); 2.3, 2.4 ($H_{CH2} : O_{=S}$) 2.6 ($H_{CH2} : F$); 4.1 ($P : N$)	-2.89	-0.04
$[Cl]^- : MC$	2.5 ($Cl : H_{N\text{-}CH3}$); 2.8 ($Cl : H_{CH3}$) 3.3 ($Cl : N$)	-0.98	-0.05
$[NTf2]^- : MC$	2.4 ($O_{=S} : H_{CH3}$); 2.6 ($O_{=S} : H_{C6H6}$) 2.9 ($N : H_{N\text{-}CH3}$); 3.6 ($N_{NTf2} : N_{MC}$)	-0.73	-0.03
$[P_{6,6,6,14}]^+ : MC$	2.4, 2.4, 2.7 ($H_{CH2} : O_{Ph}$); 3.6 ($P : O_{Ph}$)	-0.48	+0.01
$[P_{6,6,6,14}]^+ : MC : [Cl]^-$	2.5, 2.5, 2.9 ($H_{CH2} : Cl$); 4.0 ($P : Cl$) 2.4 ($Cl : H_{N\text{-}CH3}$); N/A ($Cl : H_{CH3}$); 4.3 ($Cl : N_{MC}$) 2.4, 2.7 ($H_{CH2} : O_{Ph}$); 3.9 ($P : O_{Ph}$)	-0.58	-0.02

Geometries and electronic structures calculated with B3LYP/6-311++G** model chemistry, as described in the text. ΔE for the two-species systems is the binding energy of the complex, as computed from the self-consistent field (SCF) energies of the complex relative to the isolated species. For the final entry, the three-species full IL-probe complex, ΔE is the energy of the three-species complex minus the energies of the IL complex and the isolated **MC**. More negative values indicate more favourable binding. Δq is the degree of charge transfer between species, as measured from the total charge of each species in the complex and isolated systems. Negative Δq values generally indicate net transfer of electron density from the anion to the cation or probe, except in the fifth entry, where the positive Δq indicates transfer of electron density from the probe to the cation, and the sixth (final) entry where the negative Δq is the net electron transfer to **MC**, which is coupled with a transfer of -0.09 a.u from Cl^- to $[P_{6,6,6,14}]^+$, the same as for the IL in the absence of the probe (first entry).

IL ion-ion complexation: Computed structures of the anion:$[P_{6,6,6,14}]^+$ ion pairs indicate that $[Cl]^-$ forms a tighter pair, lying 0.3Å closer to the phosphorus centre than is the case for the nitrogen centre of $[NTf_2]^-$ (Table 1). For $[P_{6,6,6,14}][Cl]$ the tetrahedral orientation of the P-C carbons allows for a clean approach of $[Cl]^-$ to the positive phosphorus centre. As $[Cl]^-$ approaches the P^+ centre it interacts also with CH_2 hydrogens, resulting in a cradle-like structure with the chloride sitting in the centre (Figure 2). The complex is characterised by moderate hydrogen bond type interactions between $[Cl]^-$ and CH_2 hydrogens and longer-range interactions between $[Cl]^-$ and the P^+ centre.[35] The chloride-phosphorus interaction, while longer range, is not believed to be of lesser importance than the chloride-side-chain interactions. The computed dipole moment of 12 D along the Cl---P axis illustrates how the Cl---P electrostatic interaction drives complexation; the computed separation of 3.8 Å at the upper limit of dipole-dipole interactions.

(a)

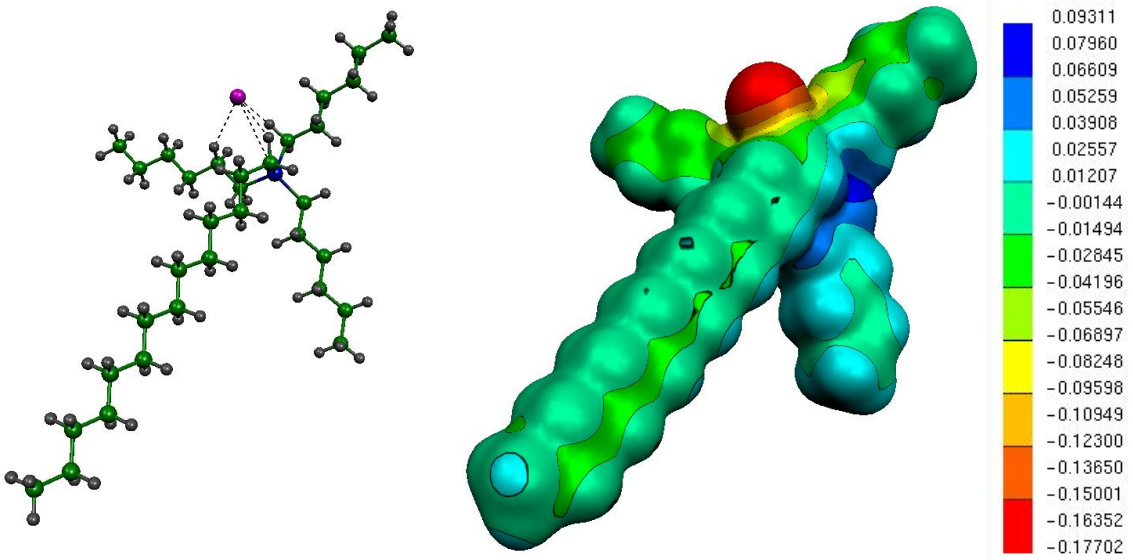

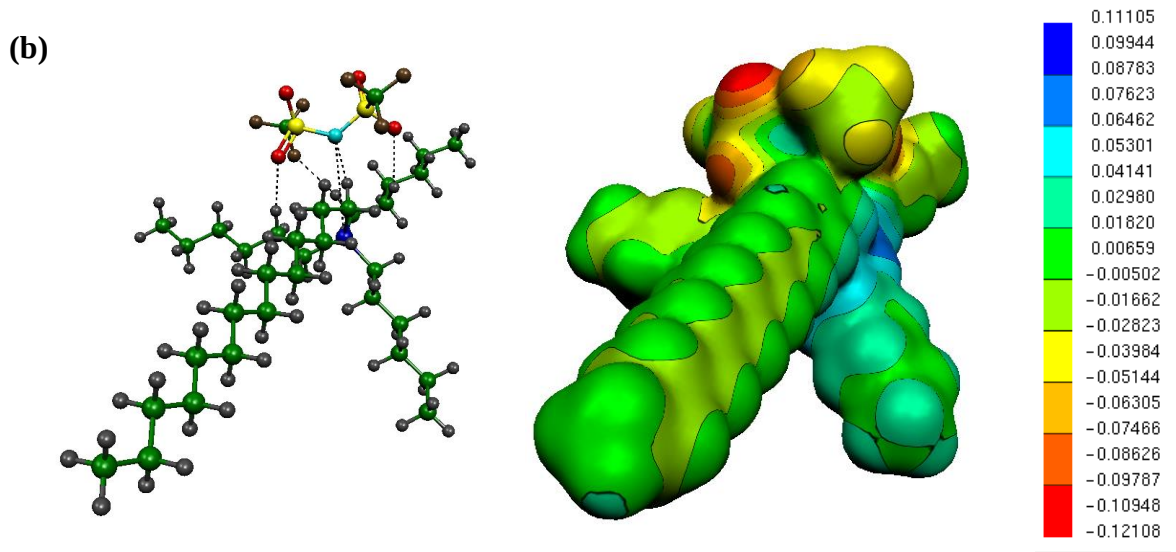

Figure 2. Complexation geometries with close contacts (the corresponding distances are given in Table 1) marked by dashed lines for net neutral phosphonium-based ILs, panel **(a)** with Cl^- and **(b)** with $[NTf2]^-$; carbon atoms are green, hydrogens grey, phosphorus atoms are blue, chlorines magenta, nitrogens cyan, oxygens red, sulphurs yellow and fluorine atoms are brown. Also shown are computed Molecular Electrostatic Potential (MEP) surfaces generated as described in the text and with surfaces coloured according to regions of net charge as marked in the scale bars, with the scale set in each case according to the largest net negative and net positive sites in each complex.

Replacing $[Cl]^-$ with the alternative $[NTf_2]^-$ anion gives significantly weaker ion pairing, the IL complexation strength decreases from -3.5 to -2.9 eV (Table 1), giving an anion-dependent liquid ion pairing energy difference ΔΔE of approximately -0.6 eV. The negative charge on $[NTf_2]^-$ is more delocalised resulting in an overall reduction in the strength and therefore effectiveness of the charge-charge interaction, compared with the single-atom $[Cl]^-$ anion (Figure 2). The significant net negative charge on the oxygens in particular allows $[NTf_2]^-$ to form more, but weaker, intermolecular interactions with the phosphonium, principally via the alkyl side-chains (Figure 2). Similar to the phosphonium chloride IL described above, moderate contacts of approximately 2.4 Å are computed for the $[P_{6,6,6,14}][NTf_2]$ complex. The similarity in intermolecular distances may therefore be attributed to the cation, with the alkyl side-chains of the cation regulating the

complexation distance in both ion pairs. The increased size of the $[NTf_2]^-$ anion restricts the approach to the phosphorus charge centre of the cation with a calculated $N^-:P^+$ distance of 4.1Å. At this distance, little or no electronic interaction can occur as reflected in the relatively low binding energy and negligible degree of electron transfer (Table 1). In common with $[P_{6,6,6,14}][Cl]$, longer-range electrostatic interactions drive complexation, as reflected in the computed dipole moment of 17 D parallel to the P---N axis of $[P_{6,6,6,14}][NTf_2]$, with shorter-range polar interactions between the anion and the phosphonium alkyl chains mediating the interaction. These calculations give a greater understanding as to why $[P_{6,6,6,14}][Cl]$ (330 ^oC) has a lower thermal stability than that of $[P_{6,6,6,14}][NTf_2]$ (420 ^oC).[36-38] Considering the structure of $[P_{6,6,6,14}][Cl]$ in Figure 2(a), the Cl^- ion is located in a favourable position (2.4 Å) to extract a hydrogen atom from one of the alkyl chains thus promoting a Hoffman like elimination mechanism for thermal decomposition at lower temperatures than that of the sterically-constrained (Figure 2b) $[P_{6,6,6,14}][NTf_2]$.[39]

Having characterised the ion pair interaction within the ILs, interactions with the open, charged merocyanine (**MC**) form of **BSP** (Figure 1a) were calculated, to probe whether the zwitterionic **MC** isomer can compete for IL ion pair interaction sites and so possibly disrupt the IL structure upon **BSP** → **MC** photoswitching.

Probe-anion complexation: In common with ion pairing in the IL, Cl^- interacts more strongly than $[NTf_2]^-$, in this case $[Cl]^-$ sits 0.2Å closer than $[NTf_2]^-$ to the N^+-CH_3 site on **MC** (Table 1), and the anions coordinate in a similar way to that observed for the interaction of the anions with the phosphonium cation in the IL pairs. The methyl hydrogens on the indoline ring play a significant role in the coordination of the anions, with contacts at ~2.4 Å as the ion associates with the positive N^+-CH_3 centre. The coordination of the anion with the methyl groups mediates the overall

interaction and stabilisation of the **MC**-anion couple (Figure 3). Natural population analysis (NPA) [30] of atomic charges gives a net charge of +0.28 on the methyl group of N^+-CH_3 compared with an average of +0.07 on the other two methyl groups, and so it is the ability of the more compact $[Cl]^-$ anion to make a strong contact with the N^+-CH_3 centre that provides the enhanced probe stabilisation with $[Cl]^-$ compared to $[NTf_2]^-$. Reference MP2 calculations given in Supporting Information confirm the general features of the probe-anion complexes and the enhanced probe stabilisation with $[Cl]^-$.

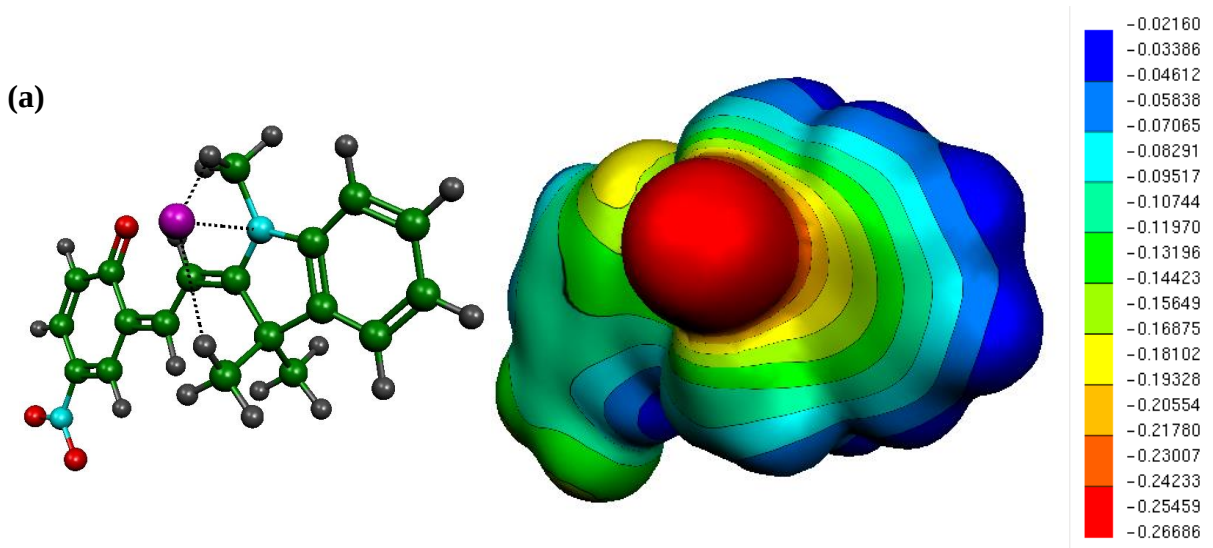

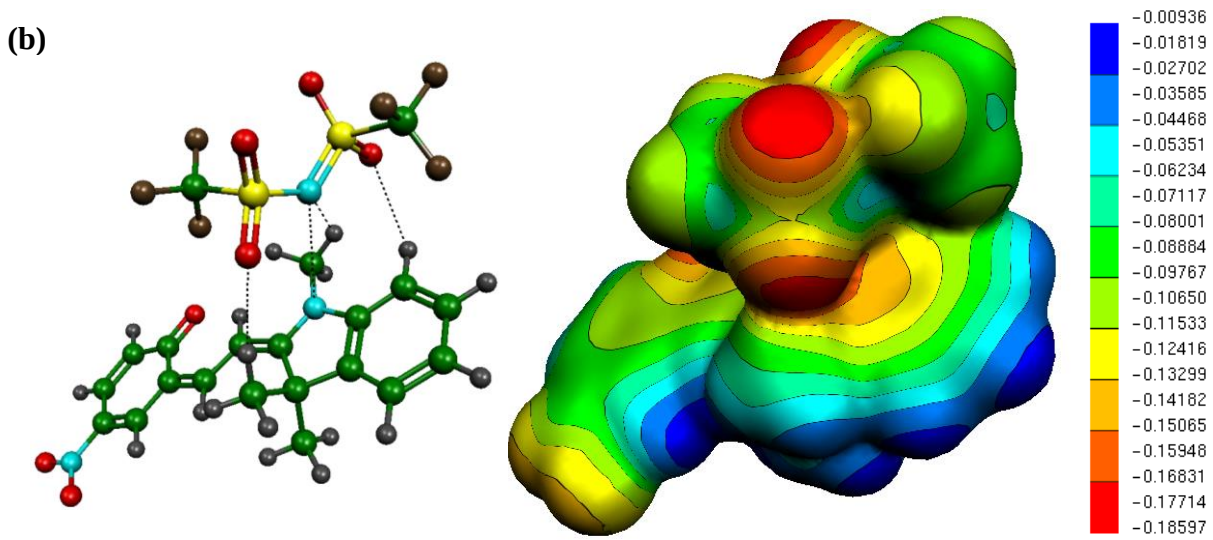

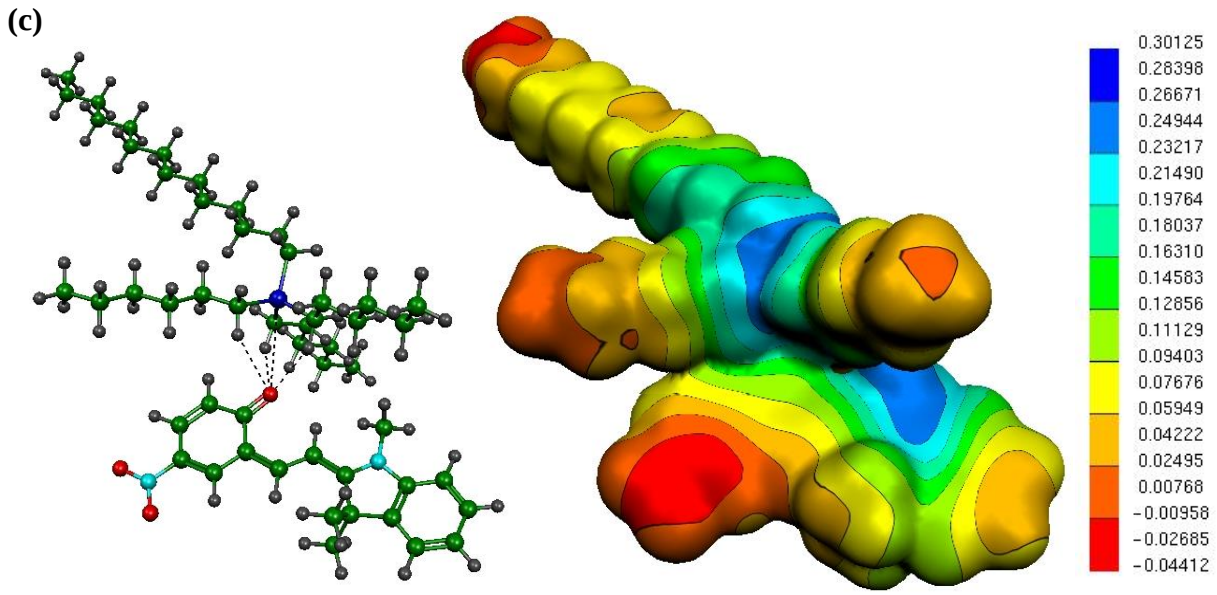

Figure 3. Complexation geometries with close contacts (given in Table 1) marked by dashed lines for charged ion-**MC** complexes, panel **(a)** the anionic complex with Cl^- and **(b)** the anionic complex with $[NTf2]^-$ and **(c)** the cationic complex with $[P_{6,6,6,14}]^+$; carbon atoms are green, hydrogens grey, phosphorus atoms are blue, chlorines magenta, nitrogens cyan, oxygens red, sulphurs yellow and fluorine atoms are brown. Also shown are computed Molecular Electrostatic Potential (MEP) surfaces generated as described in the text and with surfaces coloured according to regions of net charge as marked in the scale bars, with the scale set in each case according to the largest net negative and net positive sites in each complex.

Probe-cation complexation: The **MC**:$[P_{6,6,6,14}]^+$ complex features contact distances similar to those in $[Cl]^-$:$[P_{6,6,6,14}]^+$ (Table 1), with the $O_{(Ph)}$ bound to the **MC** phenyl ring acting as the negatively-charged centre. The strength of the interaction is weaker than for $[Cl]^-$:$[P_{6,6,6,14}]^+$, with negligible electron transfer (Table 1) and relatively weak stabilisation due to the decreased, compared with $[Cl]^-$, nucleophilicity and negative charge (-0.34 ± 0.02 a.u. averaging over all systems) of the **MC** O_{Ph} site; the phosphonium methyl H contacts to the **MC** O_{Ph} centre of 2.4 to 2.7 Å are significantly weaker than the intramolecular stabilisation due to the O---H contact of 2.2 Å within **MC**. **MC**:cation interactions are also generally weaker than **MC**:anion, due to the decreased localisation of net charge at the **MC** positive centre (Figure 1b).

Probe-anion-cation complexation: The final, and computationally most demanding, system calculated in this study is the three-species system $[P_{6,6,6,14}]^+$:**MC**:$[Cl]^-$ with the probe **MC** molecule complexed simultaneously by both IL ions. The computed structure of the complex is shown in figure 4 and summarised table 1; in general all inter-molecular contacts are weakened in the three-species complex compared with the corresponding two-species systems, particularly for ion-**MC** contacts and to a lesser extent for ion-ion contacts, giving an effective complexation energy for the full IL-probe system of -0.58 eV (Table 1), computed from the electronic energies of the three-species complex relative to the IL ion pair and the isolated probe molecule. The moderate binding energy, negligible electron transfer to **MC** and weakened intermolecular contacts all indicate that, while the zwitterionic probe is electrostatically stabilised by the presence of the IL pair, **MC** is not sufficiently polar to break the IL pair.

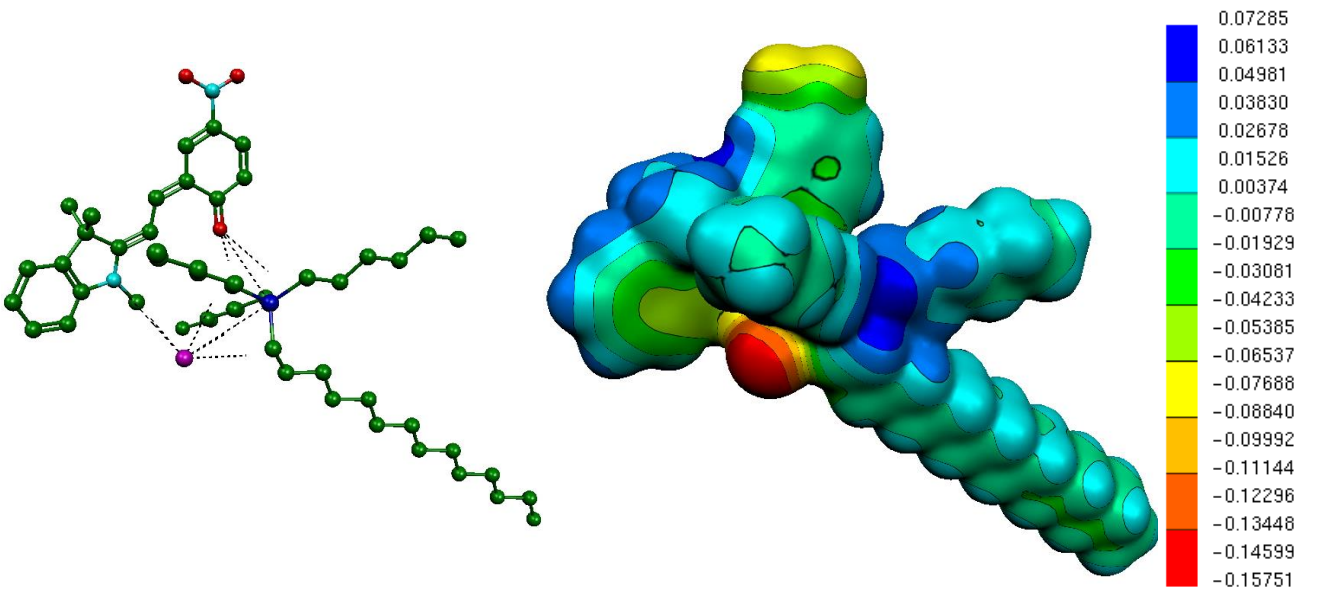

Figure 4. Complexation geometries with close contacts (given in Table 1) marked by dashed lines for the net neutral complex of MC coordinated by both ions of the phosphonium chloride IL; hydrogens are omitted for clarity (and so some contact lines appear truncated), carbon atoms are green, phosphorus atoms are blue, chlorines magenta, nitrogens cyan and oxygens red. Also shown is the computed Molecular Electrostatic Potential (MEP) surface generated as described in the text and with the surface coloured according to regions of net charge as marked in the scale bar.

This is supported by reference calculations that replaced the large phosphonium with the computationally more amenable imidazolium cation $emim^+$ and allowed computation of the influence of the IL *cation* on the full IL stabilisation of **MC**. While the detailed electronic structures will be reported as part of a larger study of emim-based ILs, the computed $emim^+$:**MC**:$[Cl]^-$ complexation energy of -0.64 eV is very similar to the phosphonium value of -0.58 eV. This suggests that, while the nature of both the cation and the anion can have a dramatic effect on inter-ion IL binding energies and to a lesser extent individual ion-**MC** interactions (Table 1), the net electrostatic stabilisation available to **MC** may not strongly depend on the nature of the IL polar headgroups. That is, a similar small amount of charge-stabilisation will be available to **MC** following inter-ion IL stabilisation, and it is the size of the non-polar region that dictates the amount of stabilisation that actually occurs.

Headgroup stabilisation vs Tail disordering: Comparison of probe stabilisation energies with known barriers to alkyl chain diffusion is instructive and indicates that the electrostatic stabilisation of the probe by the polar IL headgroups is severely penalised by the long non-polar tails of the quaternary phosphonium ion, the (putative) electrostatic interaction too weak to overcome the chain diffusion activation barrier. From previous experimental and simulation studies we may estimate the barrier to alkyl chain diffusion as 0.2 kcal/mol per CH_2 group.[40, 41] For $[P_{6,6,6,14}]^+$, this corresponds to a diffusion barrier of 6.4 kcal/mol per cation, which is just less than half the electrostatic interaction (-0.58 eV, or -13.4 kcal/mol).

Phosphonium-based ILs form a tightly-woven hydrophobic "gel", as described below, and so the tight electrostatic coupling at the probe shown in figure 4 would require significant disruption of the mesh and movement/reorientation of a large number of alkyl chains. The required relaxation

would propagate radially in three dimensions, and so we may anticipate that, for systems with such large non-polar regions, the IL nanostructuring will preclude significant **MC** stabilisation. The hydrophobic "gel" hypothesis above is supported by crystallographic studies based upon a similar structure ($[P_{10,10,10,10}][Br]$) that show significant structuring based upon side-chain interaction[42] while structural analysis of imidazolium IL structures found that the differences between solid and liquid structure results in only a small 10-15% expansion in the volume of the system.[43] Since nano-scale structuring appears to be a common characteristic of all ILs, small expansions may be expected within phosphonium ILs, preserving pseudo-crystalline ordering and thus rigidity within the liquids.

To summarise the insights obtained from the electronic structure calculations, the intra-IL ion-ion binding energy (ΔE) and extent of charge transfer (Δq) were both found to be stronger for $[P_{6,6,6,14}][Cl]$ than for $[P_{6,6,6,14}][NTf_2]$. Computed binding energies are approximately 0.5 eV higher for the chloride based IL. This value implies that the chloride based IL ion pairing interaction is much stronger, as indicated by the Walden plots in previous studies.[26, 27] Similarly, increased Δq values show a greater interaction for $[P_{6,6,6,14}][Cl]$ than for $[P_{6,6,6,14}][NTf_2]$, though both Δq values are < 0.1 a.u. (Table 1), indicating that non-covalent interactions dominate the ion-ion pairing in phosphonium-based ILs. Computed binding energies are significantly lower for **MC**-ion interactions compared to that of IL ion-ion interactions. $[Cl]^-$ again provides better stabilisation compared with $[NTf_2]^-$, with a ΔE value of -0.98eV for **MC**:$[Cl]^-$ compared with -0.73 eV for **MC**-$[NTf_2]^-$. Both **MC**-anion interactions are approximately three to four times weaker than the phosphonium-anion pairing. In addition, the differences in the energies $\Delta\Delta E$ for **MC** as a function of the anion are approximately half that calculated for the ILs. The zwitterionic **MC** probe is thus less sensitive than the IL cation to the nature of the anion. Most importantly, from the range of ΔE

values, -0.7 to -1.0 eV for **MC**-anion compared with -2.9 to -3.5 eV for the IL pair, it is clear that while **MC** coordinates the IL anion, it is unable to break the IL pair. Similarly for the **MC**-cation interaction, with **MC**-$[P_{6,6,6,14}]^+$ complexation is less than one sixth the strength of the anion$^-$-$[P_{6,6,6,14}]^+$ IL pairing. While IL-**MC** through-space interactions can stabilise **MC** in emim-based IL solvents[16], no such covalent interactions were found for the phosphonium-based ILs, that is, no high-lying occupied orbitals have significant inter-molecular character. Finally, the moderate complexation energy calculated for **MC** with both IL ions simultaneously is not expected to be sufficient to overcome the required disruption of the extended alkyl chain network in the long-tail phosphonium-based ILs, and so the IL nano-structuring is preserved; this hypothesis is supported by the calculated electronic structures, existing diffusion and Walden plot data and the experiments described below.

Measured polarity and solvatochromic effects: The electronic structures described above serve to rationalise some known features of IL structures and IL-probe interactions as described above, together with some new physicochemical experiments performed as part of this study to determine the thermal relaxation of **MC**. Taken together, the calculations and measurements help elucidate the processes at work within the ILs. **BSP** was added to each IL and irradiated to examine the immediate environment presented to the **MC** form in each liquid (Table 2). It is found that both the $[P_{6,6,6,14}][NTf_2]$ and $[P_{6,6,6,14}][Cl]$ liquids presented similar non-polar environments with a λ_{max} shift of 574nm while $E_T(30)$ values were found to vary in each liquid with values of 46.1 kcal.mol^{-1} and 43.8 kcal.mol^{-1} for $[P_{6,6,6,14}][NTf_2]$ and $[P_{6,6,6,14}][Cl]$ respectively. Such $E_T(30)$ values were expected since the stronger the ion pair, the more the binary system begins to resemble a single neutral solvent molecule. The bulkier $[NTf_2]^-$ anion resulted in less rigid associations between ion pairs and so presented more 'ideal' ionic systems with the individual ion charge becoming more

apparent than that of the $[Cl]^-$ system. The result of this is that Reichardt's Dye 30 senses a more polar environment and thus the increase in values. While the solvatochromic shifts in the same general region of ~570 nm may be attributed to the common phosphonium cation, the lack of variation may be attributed to the dependence of the interaction of the anion with the **MC**. The calculated strong interactions for $[P_{6,6,6,6,14}]^+$ with $[Cl]^-$ results in the $[Cl]^-$ becomminig somewhat imbedded between the alkyl chains of the phosphonium cation (figure 2a). As a result the anion becomes difficult for the **MC** to interact with and thus produce a stabilisation and solvatochromic effect. Although the $[NTf_2]^-$ is a bulkier anion and does not reside as close to the phosphonium cation as the $[Cl]^-$ anion, the more diffuse nature of the ion charge and the lack of any hydrogen bond donor sites removes the ability to stabilise the **MC** phenolate oxygen and the bulky nature of the anion restricts interaction with the positive region of the **MC**.

Measured thermodynamic and kinetic parameters: Samples were irradiated with sample in-situ within the cuvette holder of the spectrometer using an in-house fabricated UV LED array to induce ring opening and **MC** formation. The cuvette holder was thermostatted to ensure accurate reproducible sample heating. Upon removal of the light source**,** thermal relaxation first order decay curves were examined using equation **(1)**.

$$\ln \frac{[A]}{[A_0]} = -kt \qquad \textbf{(1)}$$

The rates of thermal relaxation were recorded at 298K and summarised in Table 2. The thermal relaxation of $[P_{6,6,6,14}][Cl]$ is almost half that of $[P_{6,6,6,14}][NTf_2]$ at 1.0 s^{-1} and 1.9 s^{-1} respectively. As with the solvatochromic parameters previously discussed, the calculated ability of the chloride ion to associate closer to the positive charge of the **MC** serves to explain the observed enhanced

stability (increased lifetime) of the open form. Similarly, the charge of the chloride ion is much more concentrated because it is a single atom. In the case of the $[NTf_2]^-$ molecule the charge is more delocalised and so the point strength of the negative charge is diminished and dispersed and so provides less counter-charge to the positive site of the **MC** zwitterion. Diminished electrostatic stabilisation therefore results in faster thermal relaxation of **MC** to its ground non-zwitterionic state. Additionally, the enhanced liquid ion pairing with $[Cl]^-$ may provide a more rigid IL network around the probe moleclue which would in turn restrict the thermal relaxation of the **MC** to its closed form.

To test this hypothesis, thermodynamic parameters were derived using equations **(2) (3)** and **(4),** providing the activation energy (E_a), entropy of activation ($\Delta S^{\ddagger}$), enthalpy of activation ($\Delta H^{\ddagger}$), Gibbs free energy of activation ($\Delta G^{\ddagger}$) and the equilibrium constant for activation ($K^{\ddagger}$) of each system (Table 1) using the Eyring equation for transition state theory.[44]

$$\ln k = E_a / RT + \ln A \qquad \textbf{(2)}$$

$$\ln(k/T) = -\Delta H^{\ddagger} / RT + \ln(k_B / h) + \Delta S^{\ddagger} / R \qquad \textbf{(3)}$$

$$k = (k_B T / h) K^{\ddagger} \qquad \textbf{(4)}$$

where,
k = rate constant
R = gas constant
T = temperature
A = pre-exponential factor
h = Planck's constant
k_b = Boltzmann constant

The resulting entropies of activation $\Delta S^{\ddagger}$ of -96.13J.K^{-1}.mol^{-1} and -14.59 J.K^{-1}.mol^{-1} for $[P_{6,6,6,14}][Cl]$ and $[P_{6,6,6,14}][NTf2]$ respectively indicate that the chloride based IL does indeed present a more rigid solvent system than that of $[NTf2]^-$ based ILs, consistent with the arguments

previously put forward by Fraser *et al* during their initial investigation into the formation of liquid ion pairing.[26] Under this hypothesis, the small size of the chloride ion drives the ion pairing that structures the IL. The quaternary nature of the cations coupled with the length of the side-chains, e.g. $[P_{6,6,6,14}]^+$, results in the formation of a hydrophobic mesh dotted with paired charged headgroups, resulting in a rigid liquid structure. **MC** is a bulky molecule which requires significant reorientation during thermal relaxation and so its conformational space may become restricted within this rigid liquid structure, prolonging the lifetime of the zwitterionic isomer. The bulkier $[NTf_2]^-$ anion means that ion pairing is weaker (Table 1) and so the formation of a more 'ideal' IL occurs, with reduced rigidity in the liquid structure, as reflected in the lower magnitudes of the measured $\Delta S^{\ddagger}$ values and lower *k* values, resulting in a faster thermal relaxation τ of the **MC** to its closed form. Similarly, lower enthalpies of activation $\Delta H^{\ddagger}$ (22.63 kJ.mol^{-1} difference) implied that for chloride based ILs the level of internal energy transferred by the relaxation process at the transition state of the **MC** is less than that of $[NTf_2]^-$. Such reductions would be expected in the more rigid chloride system where less interaction through solvent reorientation occurs between **MC** and the ions in solution. Activation energies E_a support the enthalpic and entropic parameters, with less energy required for the thermal relaxation of the **MC** to its ground state in chloride based ILs.

Table 2: Thermodynamic and kinetic parameters of **BSP** in ionic liquids. Reference values from Fraser et al.[26]

	$E_T(30)$ *(kcal.mol^{-1})*	λ_{max} *(nm)*	k_{20} *(x10^{-3}s^{-1})*	S.D *±(x10^{-5})*	E_a *(kcal.mol^{-1})*	$\Delta S^{\ddagger}$ *(J.K^{-1}.mole^{-1})*	$\Delta H^{\ddagger}$ *(kJ.mol^{-1})*	$\Delta G^{\ddagger}_{20}$ *(kJ.mol^{-1})*	$K^{\ddagger}$ *(x10^{-5})*	ΔW^{26}	$\Delta E_{disp}{}^{26}$ *(kJ.mol^{-1})*
[$P_{6,6,6,14}$][Cl]	43.8	574	1	1.04	71.51	-96.13	59.76	87.93	2.47	1.4	-46.00
[$P_{6,6,6,14}$][NTf2]	46.1	574	1.9	1.39	84.94	-14.59	82.39	86.66	7.28	0.7	0.00

Conclusions

The discovery of nano-structuring within ionic liquids (ILs) has added new depth to both the complexity of characterisation of IL solvent properties and the interpretation of the impact of this structuring upon the unique effects observed in ILs. In this paper, we investigated the formation of even smaller scale, atom-centered inter-ion interactions that mediate the formation of the nano-structures and contribute to the observed physical (viscosity) and transport properties (conductivity) within the liquids. The ability to influence structuring, and thus control the transport properties, could allow for the creation of novel liquids with more predictable properties. In the present study computed electronic structures suggest that non-covalent ion-ion electrostatic and steric interactions promote the formation of liquid ion pairs in phosphonium-based ILs. When ions have dense concentrated charges (for example, the chloride anion) tightly bound liquid ion pair systems are generated leading to liquids that exhibit atypical, off-Walden plot, IL properties. In contrast, larger molecular anions such as $[NTf_2]^-$ have a more diffuse charge distribution, which gives weaker liquid ion pairing and so a more typical IL system. In addition to this, the larger size of the anion compared to that of atomic anions such as chloride would also result in weaker interactions with the phosphonium cation. The experimental measurement of physical properties in the liquids via addition of the photo-chromic spriropyran probe molecule yielded thermodynamic and kinetic data that supported the theoretical models. Taken together the simulations and experiments indicate that the zwitterionic form of the probe is unable to significantly disrupt IL nanostructuring in phosphonium-based ILs. The moderate calculated IL-probe complexation energy is not expected to surmount the barrier to disruption of the extended alkyl chain network, a hypothesis supported by the calculated electronic structures, the new physicochemical experiments and known diffusion and Walden plot behaviour.

We may anticipate that rational engineering will allow the use of systems that incorporate the balance between polar and non-polar interactions into their molecular design. For example, IL

nanostructuring may be ruptured by (a) the introduction of more polar headgroups that would allow switching from the moderate to strong headgroup-mediated probe stabilisation coupled with (b) shorter non-polar tails to switch from the large to moderate hydrophobic tail-mediated diffusion barrier. While route (a) could possibly be controlled dynamically via *in situ* electrochemical shifts, the IL hydrophobic tails, route (b), may serve as the first point for rational design of IL solvents that strongly influence molecular photo-chromism, given that the electrostatic interactions that stabilise the zwitterionic probe also promote IL nanostructuring (in a three-site anion-zwitterion-cation "tug-of-war"). Consequently, tuning of charged sites will require careful consideration of all ion-ion and IL-probe interactions.

In summary then, while the 'ionicity' of ILs can quickly become compromised by the formation of solvent-solute interactions, a key design feature of next-generation photo-rheological systems will be the incorporation of ionic materials that can make and break multi-site interactions, in a controllable manner via switchable polar and/or non-polar interactions, to create probe-sensitive changes in conductivity and viscosity.

Supporting Information Available: Anion-**MC** complex geometries and electronic structures calculated with the MP2 method. This material is available free of charge *via* the Internet at http://pubs.acs.org.

Acknowledgements

We wish to acknowledge support for this research from the Biomedical diagnostics Institute (BDI) and CLARITY, funded by Science Foundation Ireland (SFI) under Grant Nos. 05/CE3/B754 and 07/CE/I1147. Robert Byrne acknowledges Al Robertson (Cytec Canada Inc) for helpful discussions and supply of ionic liquids. Damien Thompson acknowledges SFI for computing resources at Tyndall National Institute and SFI/ Higher Education Authority for computing time at the Irish Centre for High-End Computing (ICHEC).

References

1. Daibin, K.; Satoshi, U.; Robin, H.-B.; Shaik , M. Z.; Michael, G., Organic Dye-Sensitized Ionic Liquid Based Solar Cells: Remarkable Enhancement in Performance through Molecular Design of Indoline Sensitizers13. *Angewandte Chemie International Edition* **2008,** 47, (10), 1923-1927.
2. Singh, P. K.; Kim, K.-W.; Rhee, H.-W., Development and characterization of ionic liquid doped solid polymer electrolyte membranes for better efficiency. *Synthetic Metals* **2009,** 159, (15-16), 1538-1541.
3. Stracke, M. P.; Ebeling, G.; Cataluna, R.; Dupont, J., Hydrogen-Storage Materials Based on Imidazolium Ionic Liquids. *Energy & Fuels* **2007,** 21, (3), 1695-1698.
4. Kalhor, H. R.; Kamizi, M.; Akbari, J.; Heydari, A., Inhibition of Amyloid Formation by Ionic Liquids: Ionic Liquids Affecting Intermediate Oligomers. *Biomacromolecules* **2009,** 10, (9), 2468-2475.
5. Hallett, J. P.; Liotta, C. L.; Ranieri, G.; Welton, T., In Search of an "Ionic Liquid Effect". *ECS Transactions* **2009,** 16, (49), 81-87.
6. Hemeon, I.; Barnett, N. W.; Gathergood, N.; Scammells, P. J.; Singer, R. D., Manganese Dioxide Allylic and Benzylic Oxidation Reactions in Ionic Liquids. *Australian Journal of Chemistry* **2004,** 57, 125-128.
7. Gordon, C. M., New developments in catalysis using ionic liquids. *Applied Catalysis A: General* **2001,** 222, (1-2), 101-117.
8. Lewandowski, A.; Swiderska, A., Electrochemical capacitors with polymer electrolytes based on ionic liquids. *Solid State Ionics* **2003,** 161, (3-4), 243-249.
9. Crowhurst, L.; Falcone, R.; Lancaster, N. L.; Llopis-Mestre, V.; Welton, T., Using Kamlet-Taft Solvent Descriptors To Explain the Reactivity of Anionic Nucleophiles in Ionic Liquids. *J. Org. Chem.* **2006,** 71, (23), 8847-8853.
10. Rodrigues, F.; do Nascimento, G. M.; Santos, P. S., Studies of ionic liquid solutions by soft X-ray absorption spectroscopy. *Journal of Electron Spectroscopy and Related Phenomena* **2007,** 155, (1-3), 148-154.
11. Coleman, S. P.; Byrne, R.; Minkovska, S.; Diamond, D., Thermal reversion of Spirooxazine in ionic liquids containing the [NTf2]- anion. *Physical Chemistry Chemical Physics* **2009,** 11, (27), 5608-5614.
12. Byrne, R.; Coleman, S.; Fraser, K. J.; Raduta, A.; MacFarlane, D. R.; Diamond, D., Photochromism of nitrobenzospiropyran in phosphonium based ionic liquids. *Physical Chemistry Chemical Physics* **2009,** 11, (33), 7286-7291.
13. Reichardt, C., Solvatochromic Dyes as Solvent Polarity Indicators. *Chem. Rev.* **1994,** 94, (8), 2319-2358.
14. Figueras, J., Hydrogen bonding, solvent polarity, and the visible spectrum of phenol blue and its derivativatives. *J. Am. Chem. Soc.* **1971,** 93, (13), 3255-3263.
15. Jeliazkova, B. G.; Minkovska, S.; Deligeorgiev, T., Effect of complexation on the photochromism of 5'-(benzothiazol-2-yl)spiroindolinonaphthooxazines in polar solvents. *Journal of Photochemistry and Photobiology A: Chemistry* **2005,** 171, (2), 153-160.
16. Ipe, B. I.; Mahima, S.; Thomas, K. G., Light-Induced Modulation of Self-Assembly on Spiropyran-Capped Gold Nanoparticles: A Potential System for the Controlled Release of Amino Acid Derivatives. *Journal of the American Chemical Society* **2003,** 125, (24), 7174-7175.
17. Atabekyan, L. S., The Kinetics of Photocoloration of Spiropyrans upon Complexation. *High Energy Chemistry* **2002,** 36, (6), 397-404.
18. Chibisov, A. K.; Görner, H., Complexes of spiropyran-derived merocyanines with metal ions: relaxation kinetics, photochemistry and solvent effects. *Chemical Physics* **1998,** 237, (3), 425-442.
19. Minkovska, S.; Jeliazkova, B.; Borisova, E.; Avramov, L.; Deligeorgiev, T., Substituent and solvent effect on the photochromic properties of a series of spiroindolinonaphthooxazines. *Journal of Photochemistry and Photobiology A: Chemistry* **2004,** 163, (1-2), 121-126.
20. Byrne, R.; Fraser, K. J.; Izgorodina, E.; MacFarlane, D. R.; Forsyth, M.; Diamond, D., Photo- and solvatochromic properties of nitrobenzospiropyran in ionic liquids containing the [NTf2]- anion. *Physical Chemistry Chemical Physics* **2008,** 10, (38), 5919-5924.
21. Consorti, C. S.; Suarez, P. A. Z.; de Souza, R. F.; Burrow, R. A.; Farrar, D. H.; Lough, A. J.; Loh, W.; da Silva, L. H. M.; Dupont, J., Identification of 1,3-Dialkylimidazolium Salt Supramolecular Aggregates in Solution. *The Journal of Physical Chemistry B* **2005,** 109, (10), 4341-4349.
22. Iwata, K.; Okajima, H.; Saha, S.; Hamaguchi, H.-o., Local Structure Formation in Alkyl-imidazolium-Based Ionic Liquids as Revealed by Linear and Nonlinear Raman Spectroscopy. *Accounts of Chemical Research* **2007,** 40, (11), 1174-1181.
23. Pott, T.; Meleard, P., New insight into the nanostructure of ionic liquids: a small angle X-ray scattering (SAXS) study on liquid tri-alkyl-methyl-ammonium bis(trifluoromethanesulfonyl)amides and their mixtures. *Physical Chemistry Chemical Physics* **2009,** 11, (26), 5469-5475.

24. Canongia Lopes, J. N. A.; Padua, A. A. H., Nanostructural Organization in Ionic Liquids. *The Journal of Physical Chemistry B* **2006,** 110, (7), 3330-3335.
25. Byrne, R.; Coleman, S.; Gallagher, S.; Diamond, D., Designer molecular probes for phosphonium ionic liquids. *Physical Chemistry Chemical Physics* **2010,** 12, (8), 1895-1904.
26. Fraser, K. J.; Izgorodina, E. I.; Forsyth, M.; Scott, J. L.; MacFarlane, D. R., Liquids intermediate between "molecular" and "ionic" liquids: Liquid Ion Pairs? *Chemical Communications* **2007**, (37), 3817-3819.
27. MacFarlane, D. R.; Forsyth, M.; Izgorodina, E. I.; Abbott, A. P.; Annat, G.; Fraser, K., On the concept of ionicity in ionic liquids. *Physical Chemistry Chemical Physics* **2009,** 11, (25), 4962-4967.
28. M. J. Frisch; G. W. Trucks; H. B. Schlegel; G. E. Scuseria; M. A. Robb; J. R. Cheeseman; J. A. Montgomery, J.; T. Vreven; K. N. Kudin; J. C. Burant; J. M. Millam; S. S. Iyengar; J. Tomasi; V. Barone; B. Mennucci; M. Cossi; G. Scalmani; N. Rega; G. A. Petersson; H. Nakatsuji; M. Hada; M. Ehara; K. Toyota; R. Fukuda; J. Hasegawa; M. Ishida; T. Nakajima; Y. Honda; O. Kitao; H. Nakai; M. Klene; X. Li; J. E. Knox; H. P. Hratchian; J. B. Cross; V. Bakken; C. Adamo; J. Jaramillo; R. Gomperts; R. E. Stratmann; O. Yazyev; A. J. Austin; R. Cammi; C. Pomelli; J. W. Ochterski; P. Y. Ayala; K. Morokuma; G. A. Voth; P. Salvador; J. J. Dannenberg; V. G. Zakrzewski; S. Dapprich; A. D. Daniels; M. C. Strain; O. Farkas; D. K. Malick; A. D. Rabuck; K. Raghavachari; J. B. Foresman; J. V. Ortiz; Q. Cui; A. G. Baboul; S. Clifford; J. Cioslowski; B. B. Stefanov; G. Liu; A. Liashenko; P. Piskorz; I. Komaromi; R. L. Martin; D. J. Fox; T. Keith; M. A. Al-Laham; C. Y. Peng; A. Nanayakkara; M. Challacombe; P. M. W. Gill; B. Johnson; W. Chen; M. W. Wong; C. Gonzalez; Pople, J. A. *Gaussian 03 Revision C.02*, Gaussian Inc: Wallingford, CT, 2004.
29. Becke, A. D., Density-functional thermochemistry. III. The role of exact exchange. *The Journal of Chemical Physics* **1993,** 98, (7), 5648-5652.
30. Reed, A. E.; Weinstock, R. B.; Weinhold, F., Natural population analysis. *The Journal of Chemical Physics* **1985,** 83, (2), 735-746.
31. Izgorodina, E. I.; Bernard, U. L.; MacFarlane, D. R., Ion-Pair Binding Energies of Ionic Liquids: Can DFT Compete with Ab Initio-Based Methods? *The Journal of Physical Chemistry A* **2009,** 113, (25), 7064-7072.
32. Flükiger, P. F. *Molekel: Molecular Visualisation Software*, 4.3; University of Geneva Geneva.
33. Kaplan, I. G., *Intermolecular Interactions: Physical Picture, Computational Methods and Model Potentials*. John Wiley & Sons Ltd: Chichester, 2006.
34. Burrell, A. K.; Sesto, R. E. D.; Baker, S. N.; McCleskey, T. M.; Baker, G. A., The large scale synthesis of pure imidazolium and pyrrolidinium ionic liquids. *Green Chemistry* **2007,** 9, (5), 449-454.
35. Aakeroy, C. B.; Evans, T. A.; Seddon, K. R.; Páinkó, I., The C-H...Cl hydrogen bond: does it exist? *New Journal of Chemistry* **1999,** 23, 145-152.
36. Newman, P. J.; MacFarlane, D. R., Preparation of CdSe Quantum Dots in Ionic Liquids. *Zeitschrift für Physikalische Chemie* **2006,** 220, 1473–1481.
37. Cytec *CYPHOS IL 101 phosphonium ionic liquid*; 2/9/2005, 2005.
38. Cytec, CYPHOS IL 109 phosphonium ionic liquid. **2005**.
39. Calderon, J. U.; Lennox, B.; Kamal, M. R., Thermally stable phosphonium-montmorillonite organoclays. *Applied Clay Science* **2008,** 40, (1-4), 90-98.
40. Bain, C. D.; Troughton, E. B.; Tao, Y. T.; Evall, J.; Whitesides, G. M.; Nuzzo, R. G., Formation of monolayer films by the spontaneous assembly of organic thiols from solution onto gold. *Journal of the American Chemical Society* **1989,** 111, (1), 321-335.
41. Gannon, G.; Larsson, J. A.; Greer, J. C.; Thompson, D., Quantification of Ink Diffusion in Microcontact Printing with Self-Assembled Monolayers. *Langmuir* **2008,** 25, (1), 242-247.
42. Abdallah, D. J.; Bachman, R. E.; Perlstein, J.; Weiss, R. G., Crystal Structures of Symmetrical Tetra-n-Alkyl Ammonium and Phosphonium Halides. Dissection of Competing Interactions Leading to â€œBiradialâ€□ and â€œTetraradialâ€□ Shapes. *The Journal of Physical Chemistry B* **1999,** 103, (43), 9269-9278.
43. Dupont, J., On the Solid, Liquid and Solution Organization of Imidazolium Ionic Liquids. *Journal of the Brazilian Chemical Society* **2004,** 15, (3), 341-350.
44. Laidler, K. J.; Meiser, J. H., *Physical Chemistry*. 3rd edition ed.; Houghton Mifflin: Boston, 1999.